

Surface-assisted photoalignment in dye-doped liquid-crystal films

C.-R. Lee, T.-L. Fu, K.-T. Cheng, and T.-S. Mo

Department of Physics, National Cheng Kung University, Tainan, Taiwan 701, Republic of China

A. Y.-G. Fuh*

Department of Physics and Institute of Electro-optics, National Cheng Kung University, Tainan, Taiwan 701, Republic of China

(Received 8 August 2003; published 22 March 2004)

This study examines the surface-assisted photoalignment effect of dye-doped liquid-crystal films having a homogeneous alignment. Observations made using a polarizing optical microscope, a scanning electronic microscope, and an atomic force microscope confirm that the morphology of laser-induced surface-adsorbed dyes at the command surface strongly affects the orientation of liquid crystals (LC's) in a manner that depends significantly on the intensity and duration of the pumping. In weak-intensity regime, a homogeneous and fine layer of adsorbed dyes competes with a layer of ripple structure in reorienting LC's. These two effects dominantly cause LC's to reorient perpendicular and parallel to the polarization direction of the pump beam in the early and late stages, respectively. In the high-intensity regime, rough and inhomogeneous ribbonlike adsorbents produced by rapid and random aggregation and adsorption form on the top of the preformed microgrooves, reorienting LC's irregularly. This surface morphology does not enable photoalignment.

DOI: 10.1103/PhysRevE.69.031704

PACS number(s): 42.70.Df, 68.43.Mn, 78.68.+m

I. INTRODUCTION

The surface-assisted photoalignment effect has become particularly important in recent years because of the interesting physical mechanisms involved and its potential applications—for example, in the liquid-crystal display (LCD) industry. Conventionally, the alignment of LC's is performed by rubbing polyimide/polymer, probably causing problems involving static electricity, dust particles, and other residues on the rubbed surface. Techniques of surface-assisted photoalignment may solve these problems [1–6]. Some reports over the last decade have addressed this effect using dye-doped liquid-crystal (DDLC) films [2–6].

Although several studies, cited above, have thoroughly addressed the mechanism of the photoalignment, many aspects of this topic are not yet understood. In particular, methyl-red-(MR-) doped LC's represent a very interesting system for studying photoalignment. Normally, under proper irradiation by blue-green light, MR molecules tend to be adsorbed onto the surface of the substrate, reorienting the LC molecules into a new permanent LC configuration [3]. In 2001, Ouskova *et al.* [5,6] stated that photoalignment with LC's depends strongly on the intensity of the pump beam in a MR-doped LC system. They attributed the photoalignment effect to two mechanisms—adsorption and desorption—which dominate in strong- and weak-intensity regimes, respectively. These mechanisms tend to reorient LC molecules parallel and perpendicular to the polarization direction of the pump beam, respectively. However, their work seems to lack some important and direct observations of the surface morphology that could have been made using a scanning electronic microscope (SEM) or an atomic force microscope (AFM), and this morphology may play an important role in

LC alignment. This study focuses on the effect of the surface morphology of the adsorbed substrate on the permanent alignment of LC's using SEM and AFM to examine MR-doped LC films. The surface morphology of the adsorbed substrate is found to depend markedly on not only the intensity, but also the duration of the pumping. Three different morphologies are observed—a homogeneous and fine layer of adsorbed dyes, a layer with microgrooves, and an inhomogeneous ribbonlike and rough adsorbed layer. The first and second types of layers dominate, in the early and late stages, respectively, in the weak-intensity regime, tending to cause the LC's to reorient perpendicular and parallel to the polarization direction of pump beam. The last type of layer dominates in the strong intensity regime, possibly severely disturbing the orientation of the LC's.

II. EXPERIMENT

The LC's and azo dyes used herein are E7 (Merck) and MR (methyl red, purchased from Aldrich). The concentration of MR doped in the E7 host is ~ 1.0 wt %. Two indium-tin-oxide- (ITO-) coated glass slides, separated by two 25- μ m-thick plastic spacers, are employed to make an empty cell. An alignment film [PVA, poly(vinyl alcohol)] is coated onto one of the two ITO glass slides and rubbed. Drops of the homogeneously mixed materials are then injected into the empty cell to form a DDLC sample. LC molecules are aligned with each other near the rubbed surface (reference surface S_R) and extended through the bulk of the sample to another surface (command surface S_C) without alignment of the film. The homogeneous alignment in the DDLC sample is verified using a conoscope.

One linearly polarized (y -direction) Ar^+ laser beam ($\lambda = 514.5$ nm), with an intensity of I , serving as a pump beam, impinges onto the DDLC sample from S_C (no alignment surface). The direction of rubbing (\mathbf{R}) on S_R is along the y axis (i.e., polarization direction of pump beam). After the sample

*Author to whom correspondence should be addressed. Electronic address: andyfuh@mail.ncku.edu.tw

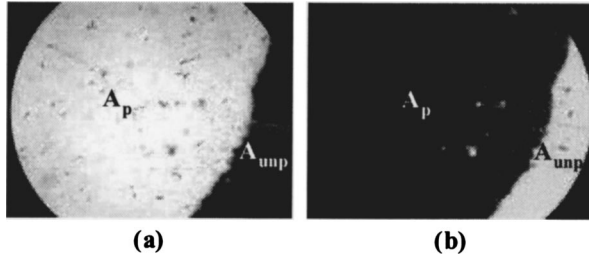


FIG. 1. (a) and (b) show images of an area near the pumped region using an optical microscope using crossed and parallel polarizers, respectively, after the DDLC sample is stimulated using an Ar ion laser ($\lambda = 514.5$ nm) at weak intensity (3 mW/cm^2) for 3 h. A_p and A_{unp} indicate the pumped and unpumped regions, respectively. The polarizer is parallel to \mathbf{R} , and the light enters the cell from S_R in the microscope.

is pumped for time t , the formed permanent LC structure is observed using a polarizing optical microscope (POM). Afterwards, the seal epoxy on the edges of the cell is removed carefully. Then the sample is submerged into the solvent, hexane, for a few minutes. The solvent works its way into the cell and gradually replaces the LC's during that period of time. Once the LC's are dissolved, the plate of the cell with S_R is removed carefully. The sample is then baked in a vacuum chamber to evaporate the solvent. In this process, the solvent is found to be effective in removing the LC's and has little deformable effect on the dye-adsorbed surface morphology on S_C . The laser-induced surface morphology in the pumped region on S_C is carefully elucidated using SEM and AFM [7].

III. RESULTS AND DISCUSSION

This work uses a linearly polarized pump beam with a very low intensity of $I \sim 3 \text{ mW/cm}^2$ to excite the DDLC sample. After a period of $t = 3$ h, the pump beam is blocked and then the pumped region is observed using a POM. Figure 1 displays the result. The polarizer is set parallel to \mathbf{R} , and white light is incident onto the sample from S_R . The terms A_p and A_{unp} represent, respectively, the pumped and unpumped regions. The region A_p is bright and dark, as shown in Figs. 1(a) and 1(b) under POM with crossed and parallel polarizers, respectively, so the formed LC structure in A_p seems to be twisted nematic (TN). The twisted angle is measured by placing the TN sample between two polarizers. The axis of the first polarizer is parallel to the rubbing direction of the sample. The transmission through the system is measured while rotating the second polarizer axis from the rubbing direction using a He-Ne laser ($\sim 1 \text{ mW}$). The angle ϕ , which gives the maximum transmission of the probe beam, gives the twisted angle, because Mauguin's condition $\Delta n d \gg \lambda$ is satisfied in the present case. The measured error of the twisted angle is $\sim 0.5^\circ$. Experimentally, the twisted angle is found to increase with increasing pumped period (the measured result is not shown). The saturated twisted angle is measured to be $\phi \sim 89^\circ$ at $t = 3$ h. This permanent TN structure is induced by the homogeneous and fine dye adsorption layer. After the MR molecules have been excited, they ex-

hibit a series of transformations, including photoisomerization, three-dimensional (3D) reorientation, diffusion, and adsorption [3]. The dye molecules finely and homogeneously adsorbed on S_C cause LC molecules to become reoriented perpendicular to the directions of polarization and propagation of pump beam, whereas the LC's near the S_R substrate align with the direction of rubbing, yielding a TN structure. Further discussion concerning the fine and homogeneous layer of adsorbed dyes will be presented later. The polarization of the incident white light through the polarizer is rotated by $\sim 89^\circ$ under the POM as the light passes through the TN bulk, because Mauguin's condition ($\Delta n d \gg \lambda$) is satisfied, yielding the results in Fig. 1. The azimuthal surface anchoring energy from the homogeneously adsorbed dyes on S_C can be written as [8]

$$W_1 = 2K_{22}\phi/(d \sin 2\phi), \quad (1)$$

where ϕ is the angle of twist, d is the cell gap, and K_{22} is the twist elastic constant. Substituting $\phi \sim 89^\circ \pm 0.5^\circ$, $d = 25 \mu\text{m}$, and $K_{22} \sim 6.5 \times 10^{-12} \text{ N}$ for E7 in Eq. (1) yields $W_1 \sim 1.5 \times 10^{-5} - 4.6 \times 10^{-5} \text{ J m}^{-2}$ for the homogeneously adsorbed surface. Referring to Ref. [2], the twisted angle is determined not only by the anchoring energy W_1 , but the dimensionless anchoring parameter $\xi = W_1 d / K_{22}$. An almost $\pi/2$ twisted angle can be achieved with $\xi \geq 10$. By substituting $W_1 \sim 1.5 \times 10^{-5} - 4.6 \times 10^{-5} \text{ J m}^{-2}$, $d = 25 \mu\text{m}$, and $K_{22} \sim 6.5 \times 10^{-12} \text{ N}$ into $W_1 d / K_{22}$, ξ is calculated to range between 58 and 177. Thus the above experimental result is reasonable.

The pumping period is extended to evaluate the rotation of LC's associated with the permanent photoalignment effect. Figures 2(a), 2(b), 2(c), and 2(d) present the pumped region under a POM with crossed polarizers for $t = 3, 10, 20$, and 40 h, respectively. The observed configuration of the sample under the POM is the same as that described above. As already shown in Fig. 1, the pumped region in Fig. 2(a) has a TN structure when t is ~ 3 h. At the center of the pumped region, a dark circle appears in the center of the beam, and the dark circle expands as the period of pumping is increased, as shown in Figs. 2(b)–2(d). These results show that another effect is initially caused at the center of the pumped region, competing with the homogeneous and fine adsorbed dyes, so the TN structure formed in the early stage shown in Fig. 2(a) is altered and eliminated. A longer pumping period corresponds to a wider altered TN region in the center. Motivated by these results, the surface morphologies in the dark and bright regions of Fig. 2(d) are examined using SEM, yielding images in Figs. 3(a) and 3(b), respectively. Clearly, a ripple structure is presented parallel to the polarization direction (y direction) of the pump beam in Fig. 3(a). In a separate experiment, the ripple structure formed in cells doped with 2 wt% and 3 wt% MR is examined. The depth of the formed microgrooves is found to be proportional to the dye concentration. Furthermore, the depth also increases with longer exposure. These results support that the microgrooves are not produced during the removal of LC from the substrates. Rather, the ripple structure in Fig. 3(a) is attributed to the laser-induced periodic adsorption of dyes.

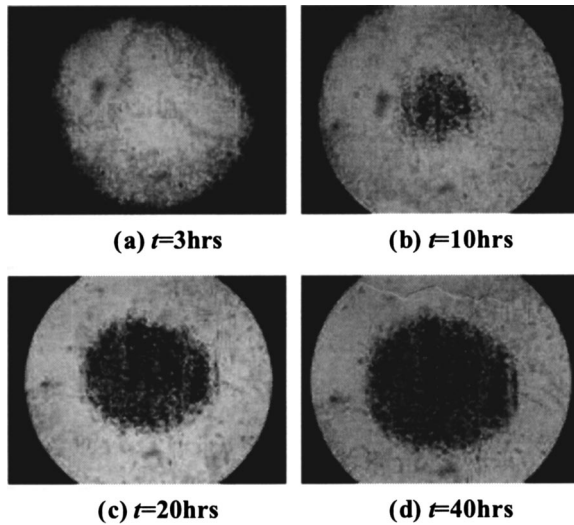


FIG. 2. Images of the pumped region of the DDLC cell excited by an Ar ion laser ($\lambda = 514.5$ nm) with an intensity of ~ 3 mW/cm² using an optical microscope with crossed polarizers during pumping periods of (a) 3, (b) 10, (c) 20, and (d) 40 h.

Although the laser-induced periodic surface structure (LIPSS) formation mechanism is very complicated and there is no sufficient explanation of the structure formation process, most researchers have accepted that the interference between the incoming polarized laser beam and its surface scattering wave plays an important role [11,13]. Accordingly, the interference between the linearly polarized pump beam and the light scattered from the dye-adsorbed surface S_C with a microscopic roughness probably causes a spatial variation of light intensity that exposes on the surface, generating a corresponding dye adsorption variation. The periodicity of the LIPSS and the ripple orientation (perpendicular or parallel to the polarization direction of pump beam) depend on parameters such as wavelength, intensity, polarization, incident angle of the pump beam, and material used. Summarizing the results of relevant LIPSS studies [9–13], two primary ripple structures can be possibly induced with different spatial spacing of $\lambda/[n(1 \pm \sin \theta)]$ (presented in pairs) and $\lambda/(n \cos \theta)$, oriented perpendicular and parallel to

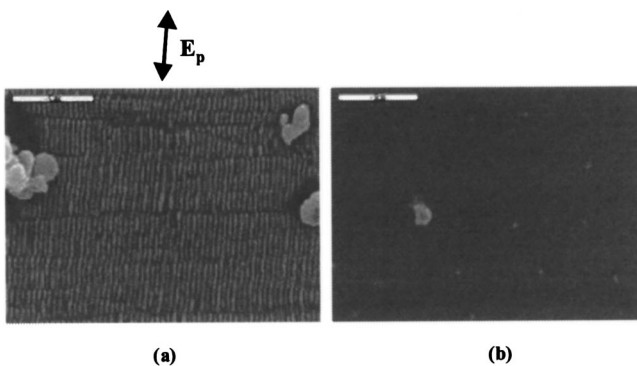


FIG. 3. (a) and (b) show SEM images of the (a) dark and (b) bright regions of Figs. 2(d), respectively. The fringe spacing in (a) is ~ 0.32 μm . The microgrooves in (a) are parallel to the pump-beam polarization \mathbf{E}_p .

the polarization of pump beam, respectively, wherein λ , n , and θ are, respectively, the wavelength of pump beam in vacuum, the refractive index of surface material, and the angle of incidence. The ripple formed in this work is parallel to the polarization of the pump beam. Thus the formula $\Lambda = \lambda/(n \cos \theta)$ possibly applies in the present case. Nevertheless, the above two formulas approximate to λ/n if θ is small. The spacing of the case discussed in the present case can be, therefore, given as

$$\Lambda \cong \lambda/n. \quad (2)$$

Substituting $\lambda \sim 0.514$ μm and $n \sim 1.6$ into Eq. (2), we obtain the spacing $\Lambda \sim 0.32$ μm , which is consistent with the experimental one (Fig. 4). The variation of the ripple structure with off-normal incidence and polarization of the pump beam will be further studied, and the result will be published elsewhere. Moreover, Figs. 4(a) and 4(b) show the obtained 2D and 3D AFM images of the ripple structure. In Fig. 4(a), dislocation lines perpendicular to the microgrooves in the ripple structure can be observed. These lines probably originate from nonuniform interfering field on the sample and correspond to the regions with weak intensity. Further study to identify the cause of these dislocation lines will be made, and the results will be reported elsewhere. Based on the obtained results, it is believed that these dislocation lines do not affect the microgrooves to align LC's along y axis in the present case. The measured average depth of the grooves in Fig. 4(c) is ~ 300 nm. Based on Berreman's theory, the azimuthal anchoring energy provided by a grooved surface is given by [14]

$$W_2 = 2\pi^3 A^2 K_{22} / \Lambda^3, \quad (3)$$

where A is the depth of the microgroove structure and K_{22} the elastic constant of the LC. Substituting $A \sim 300$ nm, $\Lambda \sim 0.32$ μm , and $K_{22} \sim 6.5 \times 10^{-12}$ N (for E7) into Eq. (3) yields $W_2 \sim 11 \times 10^{-5}$ J m⁻², which is higher than the surface anchoring energy associated with the homogeneously adsorbed dye surface, as described above ($\sim 1.5 \times 10^{-5} - 4.6 \times 10^{-5}$ J m⁻²). The LC molecules therefore reorient back in the direction parallel to \mathbf{R} , and the preformed TN structure disappears.

Figure 3(b) shows an image of a smooth surface, which induces a change of LC texture from homogeneous to TN structure [see Fig. 1(a)]. As described above, the cause is the fine and homogeneous adsorption of dyes on S_C . Some reasons support the existence of such an adsorbed layer. (i) To generate a ripple structure, a surface with an appropriate roughness must present to produce a scattering field, which then interferes with the incident light to form an interfering field. The adsorbed layer of excited MR dyes on the ITO surface of S_C offers such a roughness. (ii) The hole-burning effect in an azo-dye-doped polymer film states that, after absorbing the light, the long axes of dyes always reorient outward and are eventually perpendicular to the light polarization to minimize the free energy of the system [3]. Similarly, it is believed that the photoexcited MR dye molecules tend to reorient perpendicular to the light polarization before adsorbing on S_C in the present case. Thus the excited MR

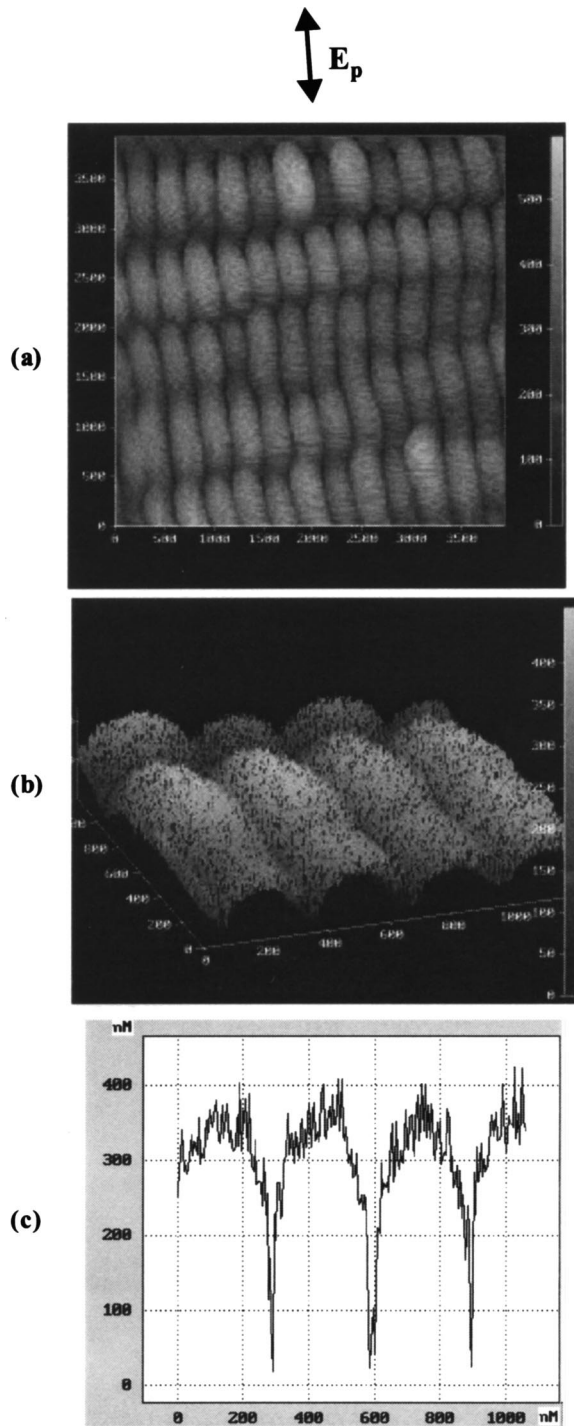


FIG. 4. (a) Two-dimensional and (b) three-dimensional AFM images of the one-dimensional ripple structure shown in Fig. 3(a). (c) The mean depth of the microgrooves in (b) is ~ 300 nm. The microgrooves in (a) are parallel to the pump-beam polarization E_p .

dyes adsorb on the surface S_C with their long axes perpendicular to the pump-beam polarization. They, in turn, align LC's to reorient perpendicular to the polarization direction of pump beam as well. Briefly, two important mechanisms compete with each other in inducing surface-assisted photoalignment in the weak intensity regime in a planar DDLC system. The homogeneous and fine dye adsorption effect dominates

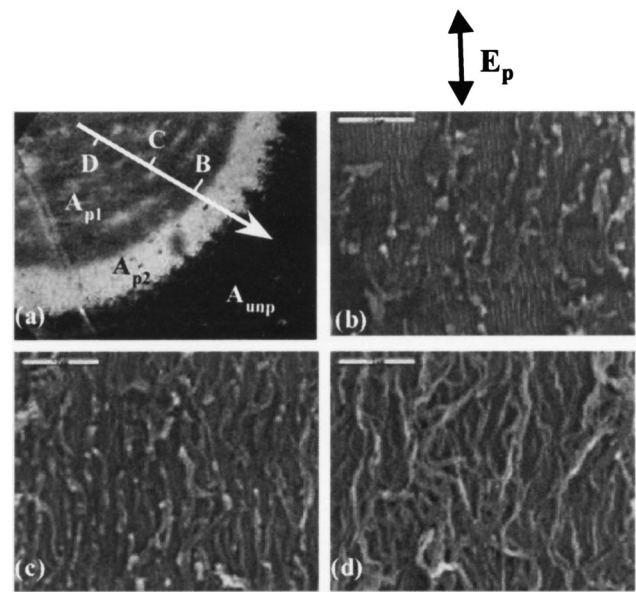


FIG. 5. (a) An image observed under an optical microscope with crossed polarizers in the pumping region after the DDLC cell is stimulated by a strong pump beam at an intensity of 80 mW/cm^2 for 3 h. A_{p1} and A_{p2} indicate the dark and bright pumped regions, respectively. A_{unp} indicates the unpumped region. (b)–(d) show SEM images of sites B, C, and D in (a), respectively. The microgrooves in (b) are parallel to the pump-beam polarization E_p .

in the early stage, while the induced ripple structure dominates in the later stage. The former and latter cause the LC molecules to reorient, respectively, perpendicular and parallel to the polarization direction of pump beam. Ouskova *et al.* [5] reported that desorption of preadsorbed dyes in the dark before pumping during irradiation of cells in the isotropic-phase-induced LC's to reorient perpendicular to the polarization direction of pump beam with a low intensity. It is believed that dark adsorption is less important than the light-induced adsorption effect in the present case. The reasons are as follows. In general, the effect of light-induced adsorption is much more significant than that of dark adsorption [3]. Furthermore, a separate experiment is performed using samples fabricated following the same conditions stated in Sec. II. The samples are placed in the dark for different durations before pumping. The evolutions of the LC texture in these samples are almost similar to the result displayed in Fig. 2 during the pumping process. Also, the time to form the ripple structure is found to be independent of the dark duration. The result that the dark-adsorbed layer does not play an essential role in reorienting LC's irradiated in the nematic phase is consistent with that reported by Voloshchenko *et al.* [2].

The effect of strongly pumped intensity on surface-assisted photoalignment is examined as follows. After an intense pump beam (80 mW/cm^2) stimulates the DDLC sample for $t = 3$ h, the pumped region is observed under a POM with crossed polarizers with the same configuration as used above. Figure 5(a) presents the obtained image. A_{p1} and A_{p2} indicate the center and periphery, respectively, of the pumped region and A_{unp} indicates the unpumped region. A_{p1} and A_{p2}

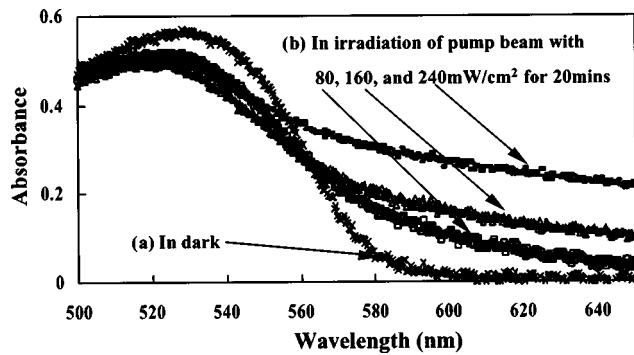


FIG. 6. Absorption spectrum of (a) a DDLC in the dark and (b) the sample after it is excited by an Ar^+ laser (green light) for various intensities.

are, respectively, dark and bright, reflecting the difference between the behaviors of LC's in these two regions. The bright periphery in A_{p2} , shown in Fig. 5(a), is similar to the image obtained in the region A_p in Fig. 1(a), which arises in the weak intensity regime (3 mW/cm^2). Figures 5(b)–5(d) present the SEM images that correspond to different pumped sites B , C , and D in Fig. 5(a). More and more ribbonlike adsorbents cover the preformed ripple structure from site B to site D at A_{p1} . These adsorbents are rough and inhomogeneous and so seem to differ from the adsorbed dyes that are observed only in the weak-intensity regime and early stage, and which are homogeneous and fine. After stimulation by a strong pump beam, the amount of excited dyes is believed to increase to excess in the DDLC sample. They rapidly aggregate and are then adsorbed onto S_C . With reference to Ref. [15], the *trans* MR molecules transform to *cis*-isomers and tend to aggregate when stimulated by green-blue light because the dipole moment of a *cis*-isomer is much stronger than that of a *trans*-isomer. Figure 6(b) indicates that, under irradiation by a strong pump beam, the absorbance of MR in the red light region greatly increases, implying that the *cis*-isomers grow quickly, and the probability that the dye aggregates significantly increases. The aligning effect of the preformed microgrooves is such that these aggregates are adsorbed effectively on microgrooves, to form ribbonlike adsorbents, as presented in Figs. 5(b)–5(d). However, these adsorbents seem to have a poor capacity to align effectively LC molecules in the direction perpendicular to the polarization direction of pump beam, because no TN structure is formed (zero twisted angle) at A_{p1} . Hence the dye molecules are believed to aggregate rapidly with irregular orientations and then be adsorbed onto S_C . These ribbonlike adsorbents cause LC's to become reoriented randomly. Figure 7(a) shows a 2D AFM image that corresponds to Fig. 5(b). Figure 7(b) shows the 3D AFM image of the region of the 1D ripple structure in Fig. 7(a). From Fig. 7(c), the mean depth of the microgrooves in Fig. 7(b) is $\sim 100 \text{ nm}$. Such a structure has an azimuthal anchoring energy of $\sim 1.2 \times 10^{-5} \text{ J m}^{-2}$, which is markedly smaller than W_2 ($\sim 11 \times 10^{-5} \text{ J m}^{-2}$) [Eq. (3)], provided by the ripple structure formed under weak intensity and in the late stage. Additionally, the ribbonlike adsorbents that form over the ripple structure prevent the growth of this structure and severely disturb the alignment of LC's. Re-

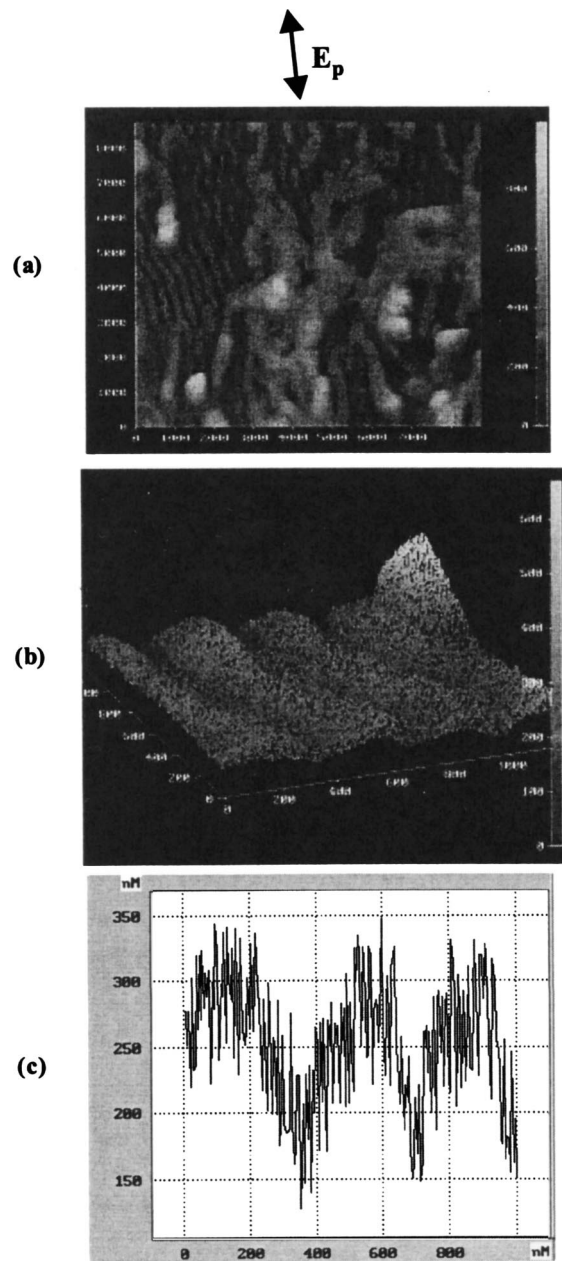


FIG. 7. (a) Two-dimensional and (b) three-dimensional AFM images of the region of the one-dimensional ripple structure shown in Figs. 5(b) and 5(c). The mean depth of the microgrooves in (b) is $\sim 100 \text{ nm}$. The microgrooves in (a) are parallel to the pump-beam polarization \mathbf{E}_p .

stated, in the strong-intensity regime, the generated surface morphologies, the shallow ripple structure, and the ribbonlike adsorbents do not promote photoalignment.

In summary, this study presents the experimental results on surface-assisted photoalignment of planar DDLC cells. New evidence obtained by POM, SEM, and AFM shows that many important surface structures induced by adsorbed dyes permanently dominate LC alignment in regimes of various intensities and/or in various time stages during pumping. Observation of the surface morphologies and calculations based on the principle of minimum surface anchoring energy indi-

cate that two different structures compete with each other in the weak-intensity regime. They are the homogeneous and fine dye adsorption layer and the layer with ripple structure, which dominantly induce LC's to be reoriented perpendicular and parallel to the polarization direction of pump beam in the early and late stages, respectively. Rough and inhomogeneous ribbonlike adsorbents form in the strong-intensity regime and are ineffective to the alignment of LC's. Photoalignment by the direct adsorption of dyes onto the ITO

surface saves the cost of the polyimide/polymer film used in the surface treatment and, hence, has possible practical uses.

ACKNOWLEDGMENTS

The authors would like to thank the National Science Council (NSC) of the Republic of China (Taiwan) for financially supporting this research under Contract No. NSC 91-2112-M-006-019.

-
- [1] W. M. Gibbons, P. J. Shannon, S.-T. Sun, and B. J. Swetlin, *Nature (London)* **351**, 49 (1991).
- [2] D. Voloshchenko, A. Khyzhnyak, Y. Reznikov, and V. Reshetnyak, *Jpn. J. Appl. Phys., Part 1* **34**, 566 (1995).
- [3] F. Simoni and O. Francescangeli, *J. Phys.: Condens. Matter* **11**, R439 (1999).
- [4] K. Ichimura, *Chem. Rev. (Washington, D.C.)* **100**, 1847 (2000).
- [5] E. Ouskova, D. Fedorenko, Yu. Reznikov, S. V. Shiyankovskii, L. Su, J. L. West, O. V. Kuksenok, O. Francescangeli, and F. Simoni, *Phys. Rev. E* **63**, 021701 (2001).
- [6] E. Ouskova, Yu. Reznikov, S. V. Shiyankovskii, L. Su, J. L. West, O. V. Kuksenok, O. Francescangeli, and F. Simoni, *Phys. Rev. E* **64**, 051709 (2001).
- [7] A. Y.-G. Fuh, M.-S. Tsai, C.-Y. Huang, T.-C. Ko, and L.-C. Chien, *Opt. Quantum Electron.* **28**, 1535 (1996).
- [8] R. Sun, X. Huang, K. Ma, and H. Jing (unpublished).
- [9] A. E. Siegman and P. M. Fauchet, *IEEE J. Quantum Electron.* **QE-22**, 1384 (1986).
- [10] S. Lugomer, *Laser Technology: Laser Driven Processes* (Prentice Hall, Englewood Cliffs, NJ, 1990).
- [11] Jeff F. Young, J. S. Preston, H. M. Van Driel, and J. E. Sipe, *Phys. Rev. B* **27**, 1155 (1983).
- [12] M. Bolle and S. Lazare, *J. Appl. Phys.* **73**, 3516 (1993).
- [13] Q.-H. Lu, Z.-G. Wang, J. Yin, and Z.-K. Zhu, *Appl. Phys. Lett.* **76**, 1237 (2000).
- [14] D. W. Berreman, *Phys. Rev. Lett.* **28**, 1683 (1972).
- [15] W. Urbach, H. Hervet, and F. Rondelez, *J. Chem. Phys.* **83**, 1877 (1985).